Ultimate Strength Of Box Beams Strengthened In Different Toque-To-Shear Ratios With CFRP Sheets

Shengqiang Ma, Norazura Muhamad Bunnori* & Kok Keong Choong

School of Civil Engineering, Universiti Sains Malaysia, Engineering Campus, NibongTebal, 14300, Penang, Malaysia

Corresponding Author: cenorazura@usm.my

Abstract: An experimental investigation and derived equations of ultimate torque on reinforced concrete (RC) box beams strengthened by carbon fiber-reinforced-polymer (CFRP) sheets subjected to combinedl torsion and shear have been carried on research. In this experiment, eight box beams were cast and separated into two groups according to two different torque-to-shear ratios (i.e., 1.597 and 2.556). Three box beams from each group strengthened by CFRP in different configurations and one control box beam were tested. The main parameters of this experiment were the different ratios and configurations, including U-jacket layers and U-jacket strips with or without longitudinal strips. The cracking pattern, failure mode, effect of wrapping schemes, torsional capacity, and behavior of the various torque-to-shear ratios were studied in detail. In terms of the variable-angle truss model and mode-2 type of failure as well as shear flow and equilibrium of forces and moment, the equations for calculating the ultimate torque of the box beams strengthened by CFRP sheets were derived. According to existing experimental results, the experimental and calculational values show a close agreement

Keywords: *Box beam, ultimate strength, torque-to-shear ratios, carbon fiber reinforced polymer (CFRP).*

1.0 Introduction

Nowadays, the methods of strengthening beams with fiber-reinforced-polymer (FRP) sheets have been widely accepted and employed around the world. Based on theoretical and experimental studies, reinforced concrete (RC) beams retrofitted in flexural and shear have made a significant progress and achievement (Chen *et al*., 2012; Baggio *et al*., 2014;Attari *et al*., 2012; Dong *et al*., 2013). However, only several studies devoted much attention to torsional strengthening; most studies were on rectangular beams fully wrapped with FRP (Al-Mahaidi and Hii, 2007; Chalioris, 2007; Ghobarah *et al*., 2002; Panchacharam and Belarbi, 2002). To the best knowledge of the authors, Meng and Grünberg (Meng and Grünberg, 2006) conducted the first experiment related to box

beams strengthened with extending a U-jacket CFRP strip to the surface of the beams under combined actions. They also proposed a mechanical model (Meng *et al*., 2007) with 37 independent equations and 37 unknowns determined by a complicated iterative algorithm, which is quite unsuitable for design purposes. Therefore, obtaining more practical and deriving simple calculative equations are necessary to determine the ultimate strength of box beams strengthened by CFRP under different torque-to-shear ratios.

In this study, based on variable-angle truss model theory and mode-2 type of failure (Krishna, 2003), the equations for calculating the ultimate torque and shear of RC box beams strengthened by CFRP sheets were derived. To do this, an experimental study (Ma *et al*., 2015) on the behavior of RC box beams strengthened by CFRP sheets under torque and shear combined actions has conducted in the structural lab of Universiti Sains Malaysia. Eight RC box beams were cast and grouped into two parts subjected to two different torque-to-shear ratios (i.e., 1.597 and 2.556). In each group, three box beams were strengthened with CFRP in different configurations, such as U-jacketing strips and U-jacketing strips with longitudinal strips within three faces. The objectives of this study are to investigate the behavior of the strengthened box beams, evaluate the effectiveness of the configuration of CFRP and the feasibility of strengthening, meanwhile, to establish ultimate torque and shear equations, according to the test results of box beams strengthened by CFRP in torsion and shear combined actions.

2.0   Experimental Program

Eight scaled RC box beams with a 350 mm × 400 mm hollow cross-section and 2,500 mm length were cast for this test. The beams were separated into two groups (groups 1 and 2) with four box beams in each group according to loading lever arm lengths of 250 and 400 mm, which can provide two different torsional moment-to-shear ratios. The ratios were 1.597 and 2.556, respectively. The control beams and the beams strengthened by CFRP had the same longitudinal and stirrups steel configuration

2.1   Materials

Ordinary Portland cement was utilized in this experiment. The compressive strength of the concrete obtained by testing a cubic cured for 28 d is shown in Table 1. The yield strength of stirrups R6 and R8 was 392 and 398 MPa, respectively. The yield strength of top longitudinal bar R10 and bottom bar T16 was 520 and 570 MPa. The CFRP applied in the test was LaMaCo composite that includes MBrace reinforcing fabric and MBrace epoxy. The properties of CFRP sheets and the epoxy were provided by the supplier. The employed CFRP had a tensile strength of 4,900 MPa, modulus of elasticity of 230 GPa, thickness of 0.117 mm, and ultimate elongation of 1.8%. The properties of the epoxy

included tensile strength of 54 MPa, modulus of elasticity of 3,435 MPa, and ultimate elongation of 3.5%.

2.2   *Specimen Characteristics and CFRP Strengthening Configuration*

The experimental specimens were designed distinctively because of the focus on torque and shear in the research zone of 1,500 mm. The details on the dimensions and reinforcement arrangement of the box beams are presented in Figure 1. The box beam was 2,500 mm long, 400 mm wide, and 350 mm high. The width of the two sides' web and the top thickness were all 50 mm, and the thickness of the bottom was 60 mm. For all the specimens, closed stirrups with 6 mm diameter were spaced at 100 mm centers in the research zone, and a closed stirrup with 8 mm diameter and 50 mm centers was used at the left side of the 1000 mm mark to make sure that this side is stronger than the research zone. 16 and 10 mm longitudinal bars were placed separately at the bottom and top flanges. Eight RC box beams were cast and separated into two groups according to two different torque-to-shear ratios. Each group had one control beam and three beams strengthened by CFRP.
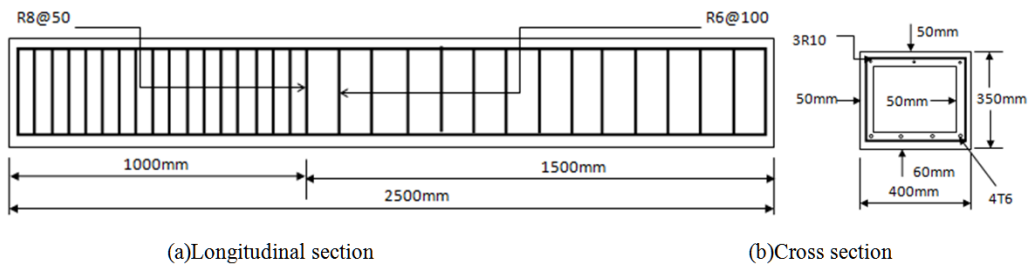

(a)Longitudinal section   (b)Cross section

Figure 1: Details on the dimensions and reinforcement arrangement of the box beams

(a)wrapped in one layer strips
(1BBS and 2BBS)

(b) wrapped in one layer strips with one layer
longitudinal strip (1BBSL1 and 2BBSL1)

(c) wrapped in two layer strips with one layer
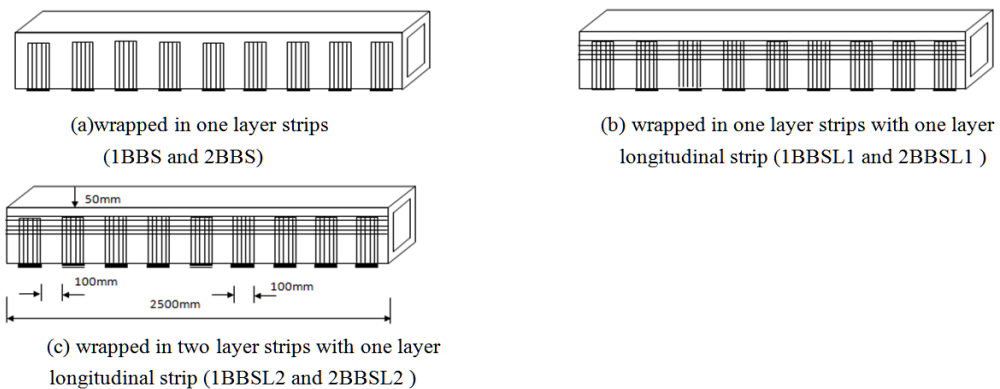longitudinal strip (1BBSL2 and 2BBSL2)

Figure 2: Schematic of the strengthened box beams

The strengthening configurations of the three beams are shown in Figure 2. In the labels 1BBC and 2BBC, the head numbers "1" and "2" represent group 1 and group 2, respectively. In the labels 1BBSL1 and 1BBSL2, the last numbers represent one layer and two layers of U-jacketing CFRP strips, respectively. The three faces of all the beams were strengthened by 100 mm U-jacket strips at 100 mm spacing along the length of the beams because it is impossible to access the top face of the bridge deck or the floor slab. 1BBS and 2BBS were only strengthened by a layer of U-jacket strips. A one-layer longitudinal strip was utilized in 1BBSL1, 2BBSL1, 1BBSL2, and 2BBSL2 to suppress the endings of the U-jacket strips and provide a nondestructive anchorage, which is expected to prevent the U-jacket strips from debonding prematurely. 1BBSL1 and 2BBSL1, as well as 1BBSL2 and 2BBSL2, have one and two layers of U-jacket strips with a layer of the longitudinal strip, respectively.

2.3   Test Setup and Instrumentation

A test setup was created to provide shear and torsion with one hydraulic actuator. The beam's two ends were supported; the right end was fixed, and the left end was allowed to rotate to produce torsional moment for the 1.5 m research zone from the right end of the beam. A designed equipment that includes a 1.2 m-long lever arm was installed 1.5 m from the right end of the beam. A 400 KN capacity hydraulic actuator supplied load to the lever arm. Moving the hydraulic actuator tip along the lever arm provided different distances between the tip and the centroidal axis of the beam and thus generated various torque-to-shear ratios. The two distances considered were 250 and 400 mm between the tip and the axis of the box beam. Two linear variable displacement transducers (LVDTs) were installed at the bottom of the beams to measure the transverse twist. Strain gauges were closely stuck on the stirrups and CFRPs. The setup of the test instrumentation is presented in Figure 3.

Figure 3: Photograph of the instrumentation

3.0   Experimental Results

3.1   *Improvement in Shear and Torque Capacity*

Table 1 shows the shear and torque capacity of the CFRP-strengthened beams and the control beams in two different torque-to-shear ratios. Data from the two groups show that the cracking capacity of the strengthened beams did not increase remarkably; the best torsional increases are 11.7% and 14.1% in 1BBSL1 of group 1 and in 2BBSL2 of group 2, respectively. However, the torque capacity of the strengthened beams improved significantly in the last stage. The maximum torsional increments are 51.8% and 34.3% in group 1 and group 2, respectively. The ultimate twist angles of the beams in group 1 almost have the same value, but a slight increase was observed in the strengthened beams in group 2. This observation verifies the conclusion that an increase in torque-to-shear ratio decreases torsional stiffness, which is defined as the ratio between torque and the angle of twist (Deifalla and Ghobarah, 2010). Compared with the strengthened beams without longitudinal strips, the longitudinal CFRP strips bonded to the endings of the U-jacket strips delayed failure, enhanced the ultimate capacity, and changed the failure mode from U-jacket strip debonding to longitudinal CFRP strip rupture.

Table 1: Cracking and ultimate shear and torque of the two groups

	Beam	Concrete Compressive Strength	Torque to shear ratio η	Cracking shear P_{cr}	Cracking torque T_{cr}	Increase in T_{cr} (%)	Ultimate shear P_{ue}	Ultimate torque T_{ue}	Increase in T_{ue} (%)	Twist angle ψ_{ue}
		MPa		(kN)	(kN.m)		(kN)	(kN.m)		(°)
Group 1	1BBC	43.40	1.579	19.94	12.6		54.8	34.63	-	2.40
	1BBS	46.40		20.1	12.7	0.8	72.93	46.08	33.1	2.60
	1BBSL1	42.40		22.27	14.08	11.7	77.2	48.78	40.9	2.50
	1BBSL2	54.50		22	13.9	10.3	83.21	52.58	51.8	2.40
Group 2	2BBC	50.20	2.556	15.77	16.12		41.2	42.12	-	2.60
	2BBS	56.70		16.04	16.4	1.7	47.65	48.72	15.7	3.10
	2BBSL1	55.00		17.72	18.12	12.4	52.46	53.64	27.4	4.60
	2BBSL2	53.70		18	18.4	14.1	55.32	56.56	34.3	4.57

The ultimate shear and torque capacity of the strengthened box beams in group 1 was enhanced more notably than that in group 2. This result can explain why U-jacket CFRP strips are more effective in strengthening box beams with a decrease in torque-to-shear ratio or why U-jacket CFRP strips are less efficient in strengthening beams under torsional action. The increase in the ultimate strength of the strengthened box beams is not proportional to the increase in the ultimate strength of the CFRP strip layers. As shown in Table 1, the ultimate torque of 1BBSL2, 1BBSL1, 2BBSL2, and 2BBSL1 improved by 51.8%, 40.9%, 34.3%, and 27.4%, respectively.

3.2   Crack patterns and failure modes

Given that the box beams were subjected to a combination of shear and torsion, two vertical webs showed different mechanisms called shear torque counteract side and shear torque added side. The shear flows of the two sides have subtractive and additive relationships between shear and torque. The test observation on the crack patterns of 1BBC and 1BBSL1 showed failure, as illustrated in Figure 4. The number of cracks in the shear torque added side was significantly greater than that in the counteract side; the cracking width was also wider. Spiral diagonal cracks mainly appeared on the three sides, namely, shear torque counteract side, added side, and the top. Comparison of the crack stretching drawing of non-strengthened beam 1BBC and CFRP-strengthened 1BBSL1 shows that the cracks in 1BBSL1 are well-distributed and that the width is obviously narrow. The ultimate strength of the beams retrofitted by CFRP improved and the distribution of stress was more even in the beams.

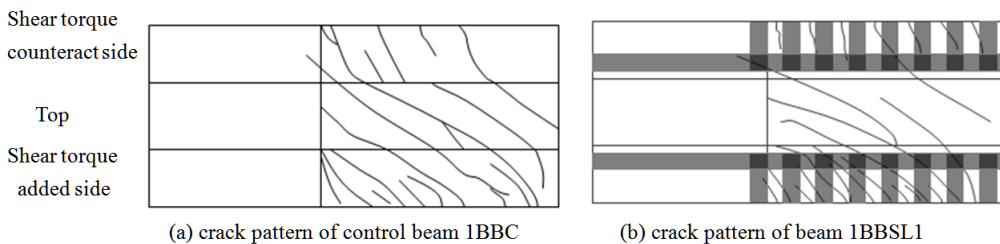(a) crack pattern of control beam 1BBC   (b) crack pattern of beam 1BBSL1

Figure. 4: Crack patterns

The control beams of the two groups exhibited torsional failure modes with spiral diagonal cracks, but the cracking angle of control beam 1BBC was smaller than that of control beam 2BBC. This result indicates that the cracking angle was caused by the increase in torque-to-shear ratio and that the strengthened specimens in these two groups followed the same cracking pattern as that in the control ones. However, the retrofitted box beams showed different failure mechanisms. Figure 5 shows the failure patterns of the U-jacket strips with and without longitudinal strips. According to the failure mechanisms, two main patterns of failure were observed from the experimental investigation. For beams that were wrapped only by U-jacket strips, debonding governed the failure. However, a longitudinal CFRP rupture existed in the beams wrapped by U-jacket strips with longitudinal strips. Therefore, the longitudinal strip confined the U-shaped strips to avoid debonding in the ultimate state and thus allowed for the improvement of ultimate torque. As for the strengthened beams, diagonal shear and torsional cracks occurred and widened in cut-through unwrapped and wrapped positions on the beams within CFRP debonding or rupture.
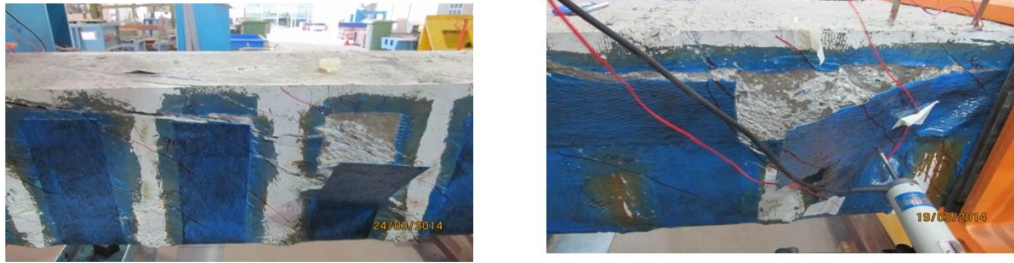
Figure 5. Two main patterns of failure: debonding and rupture

3.3   Torsional Behavior

Figure 6 shows the curves of torque versus the twist angle of the beams between two beams obtained from two groups throughout the loading period until failure occurred; two groups were included in the test for a typical comparison. Table 1 shows that the increments in the torque of 1BBS and 1BBSL2 are 33.1% and 51.8% compared with control beam 1BBC. However, the peak twist angle of the control beam and the strengthened beams had a slight difference. As shown in Figure 6(a), the three peak angles of 1BBC, 1BBS, and 1BBSL2 corresponding to the ultimate torsional moment are 2.42°, 2.57°, and 2.73°, respectively. Figure 6(b) shows the curves of the relationship of torque and twist angle. The twist angle increased in all the strengthened beams in group 2. For instance, the peak twist angle of control beam 2BBC was approximately 2.59°, whereas that of beam 2BBS, which was retrofitted with a layer of U-jacket CFRP, was 3.1°. An increase in peak twist angle was observed in beams 2BBSL1 and BBSL2; the values were 4.60° and 4.57°, respectively. Compared with the same configuration of the CFRP-strengthened beams but with different torque-to-shear ratios, the peak twist angle of 2BBSL2 was higher than that of 1BBSL2 despite the two beams having almost the same value of ultimate torque. With regard to ultimate strength, the increase in the torsional moment-to-shear ratio resulted in a decrease in total load resistance and vertical displacements and an increase in peak twist angle.
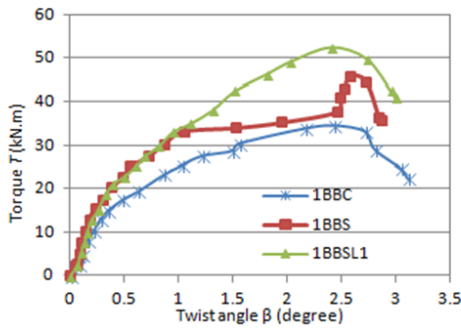
(a) Group 1(T/VB=1.5797)
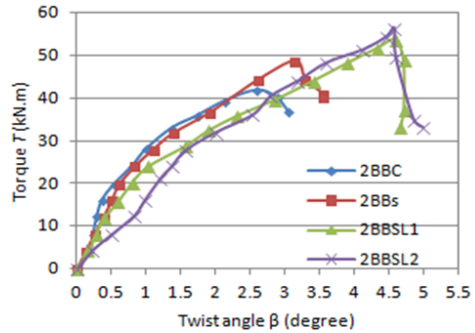
(b) Group 2(T/VB=2.556)
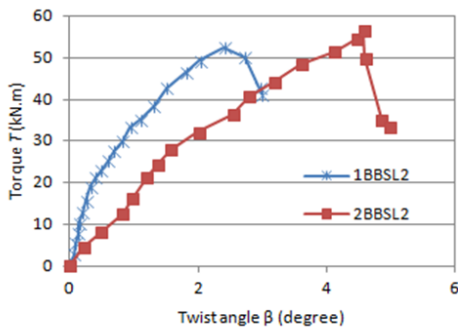
(c) Comparison between two groups

Figure 6. Curves of torque to twist angle

3.4   *Stirrup Strain and CFRP Strain.*

Figure 7(a) shows the stirrup strain versus shear. The steel strain in group 2, which had a higher torque-to-shear ratio, was larger than that in group 1 and produced steel yield. Although the shear in group 2 was smaller than that in group 1, the torsional behavior revealed more strength of transverse steel in the beam. However, to stirrup strain, no clear law was observed between the strengthened box beam and the control box beam in the same torque-to-shear ratio.

U-jacket strip strain versus torque is illustrated in Figure 7(b). All the strains of the beams (1BBSL1 and 2BBSL1) strengthened by U-jacket strips with longitudinal strips were clearly larger than the strains of the beams strengthened by only U-jacket strips because of the longitudinal strips restricting the U-jacket strips from debonding when the beams failed. Using longitudinal strips makes U-jacket strips more effective in strengthening box beams under a combined action.
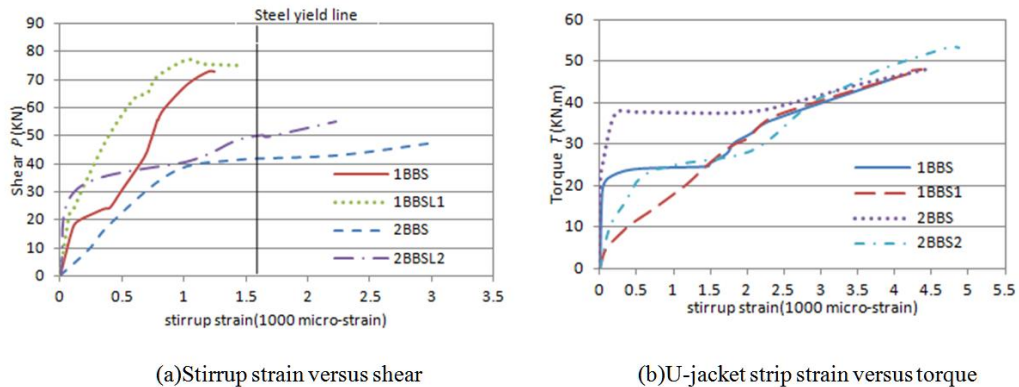
(a)Stirrup strain versus shear   (b)U-jacket strip strain versus torque

Figure 7. Stirrup and U-jacket strip strain

4.0   Calculational Equations of Ultimate Torque

4.1   Shear Flow of Each Box Wall

The angle of inclination of concrete struts was first raised by Lampert and Thurlinmann (Lampert, 1968). They made the assumption that inclinational angle may deviate from 45°, and longitudinal and transverse steel with different percentages are both yield-at-failure, which is taken as the theory of variable-angle truss model. Given that plasticity is assumed at failure, it can also be called the plasticity truss model (Hsu and Mo, 1985). Therefore, after the growth of diagonal cracks in the beam under combined action, diagonal concrete struts in each face of the beam were generated, and inclined at an angle θ to the longitudinal reinforcement. θ is a variable value with the variation of longitudinal and stirrup steel bars. Based on the variable-angle truss model and the basic equilibrium of inner and outer forces, the ultimate equations can be deduced accordingly. The variable-angle truss model of the box beam subjected to combined action is illustrated in Figure 8. The counterparts of the concrete strut diagonal forces of each wall of the beams are D_1, D_2, D_3, and D_4, and the diagonal angles are θ_1, θ_2, θ_3, and θ_4, respectively. Applied torsion T_s induces positive shear flow q_t, which circulates around the specimen in a counterclockwise direction. The shear flow produced by applied torque is $q_t = T_s/(2A_{cor})$, where A_{cor} is the circular area closed by shear flow central line. Shear V_s also produces a shear flow distribution along the centerline of the shear flow zone, as shown in Walls 1 and 3. Shear V_s generates shear flow $q_v = V_s/(2h_{cor})$, where h_{cor} is the depth of the shear flow. Therefore, the shear flows T_s and V_s are additive in Wall 1 and subtractive in Wall 3, but the shear flow in Walls 2 and 3 is only considered to have been formed by T_s. The equations of shear flow of the four walls are listed in Eq. 1.
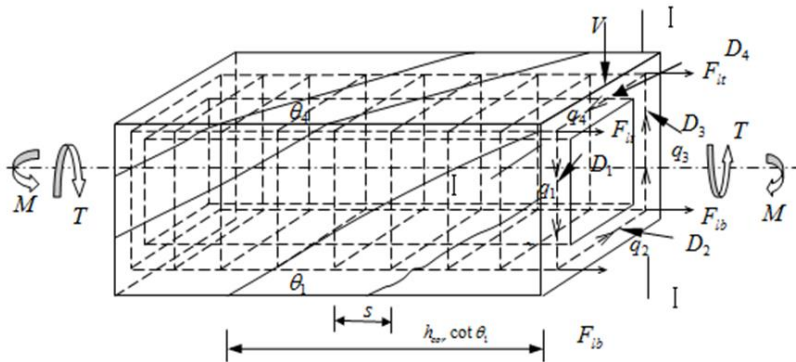
Figure 8: Variable-angle truss model of the box beam under shear, torsion, and bending moment

$$q_1 = q_t + q_v = \frac{T_s}{2A_{cor}} + \frac{V_s}{2h_{cor}} \tag{1a}$$

$$q_3 = q_t - q_v = \frac{T_s}{2A_{cor}} - \frac{V_s}{2h_{cor}} \tag{1b}$$

$$q_2 = q_4 = q_t = \frac{T_s}{2A_{cor}} \tag{1c}$$

4.2   Equilibrium of the Force Equations

The force of single stirrup F_s in the each wall was obtained from yielding the stirrup bar when the beam is close to failure; hence, the force value is identical in each wall. As a beam is strengthened by FRP, transverse and longitudinal FRP will be forced accordingly under combined action, and their strength F_{fl} and F_{fs} will be induced by the effective strain of the fibers (Ameli and Ronagh, 2007; Chalioris, 2008; Ghobarah *et al.*, 2002). Based on the force equilibrium shown in Figure 9, the equilibrium of the force equations (Jing and Grünberg, 2006) is presented as follows:

When $i = 1,3$

$$D_i \sin \theta_i = q_i h_{cor} \tag{2}$$

$$q_i h_{cor} = \frac{F_s h_{cor} \cot \theta_i}{s} + \frac{F_{fs} h \cot \theta_i}{s_f} = \frac{f_v A_v h_{cor} \cot \theta_i}{s} + \frac{f_{fs} A_{fs} h \cot \theta_i}{s_f} \tag{3}$$

When $i = 2, 4$

$$D_i \sin \theta_i = q_i b_{cor} \qquad (4)$$

$$q_2 b_{cor} = \frac{F_s b_{cor} \cot \theta_2}{s} + \frac{F_{fs} b \cot \theta_2}{s_f} = \frac{f_v A_v b_{cor} \cot \theta_2}{s} + \frac{f_{fs} A_{fs} b \cot \theta_2}{s_f} \qquad (5)$$

$$q_4 b_{cor} = \frac{F_s b_{cor} \cot \theta_4}{s} = \frac{f_v A_v b_{cor} \cot \theta_4}{s} \qquad (6)$$

where b is the width of the beam, s is the depth of the beam, b_{cor} is the width of the shear flow, s is the spacing of the stirrup, s_f is the spacing between the centerline of FRP, f_v is the strength of the stirrup, f_{fs} is the strength of the FRP strip, A_v is the area of the stirrup, A_{fs} is equal to $w_f t_f$ or the area of the FRP strip, w_f is the width of the FRP strip, and t_f is the thickness of the FRP strip.
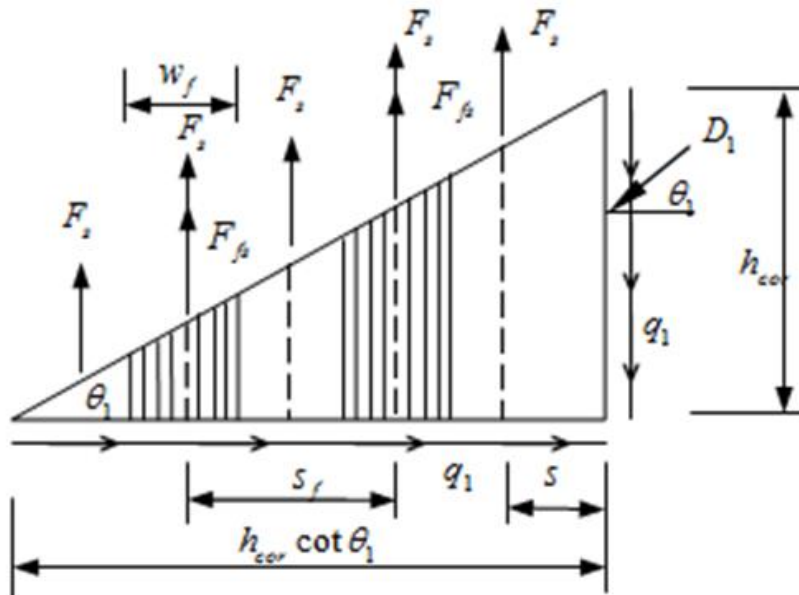

Figure 9. Free body diagram of force equilibrium

From Eqs. (1) to (6) and by neglecting the difference between h and h_{cor} and between b and b_{cor}, the variable angles can be induced as follows:

$$\cot\theta_1 = \left(\frac{T_s}{2A_{cor}} + \frac{V_s}{2h_{cor}}\right)\frac{ss_f}{f_v A_v s_f + f_{fs} A_{fs} s} \tag{7a}$$

$$\cot\theta_2 = \left(\frac{T_s}{2A_{cor}}\right)\frac{ss_f}{f_v A_v s_f + f_{fs} A_{fs} s} \tag{7b}$$

$$\cot\theta_3 = \left(\frac{T_s}{2A_{cor}} - \frac{V_s}{2h_{cor}}\right)\frac{ss_f}{f_v A_v s_f + f_{fs} A_{fs} s} \tag{7c}$$

$$\cot\theta_4 = \left(\frac{T_s}{2A_{cor}}\right)\frac{s}{f_v A_v} \tag{7d}$$

4.3   Moment Equilibrium Equations

The failure of the beams in this experiment was investigated. Torsional behavior was counted to be primary over flexural behavior. Mode-2 type of failure (Krishna, 2003) characterized by the compression zone skewed to the side of the member generally occurred; this type of failure is also referred to as lateral flexural failure. For the moment equilibrium at the $I-I$ axis, the equilibrium equation is obtained as:

$$F_{lb}b_{cor} + F_{lt}b_{cor} + f_{fl}A_{fl}b_{cor} - D_1\cos\theta_1 b_{cor} - \frac{1}{2}D_2\cos\theta_2 b_{cor} - \frac{1}{2}D_4\cos\theta_4 b_{cor} = 0 \tag{8}$$

Based on Eqs. (2) to (7), D_i and θ_i can be eliminated, and $A = \dfrac{ss_f}{f_v A_v s_f + f_{fs} A_{fs} s}$ can be replaced. Then, the equilibrium equation is derived as:

$$f_{lb}A_{lb}b_{cor} + f_{lt}A_{lt}b_{cor} + f_{fl}A_{fl}b_{cor} - \left(\frac{T_s}{2A_{cor}} + \frac{V_s}{2h_{cor}}\right)^2 b_{cor}^2 A - \frac{1}{2}\left(\frac{T_s}{2A_{cor}}\right)^2 b_{cor}^2 A - \frac{1}{2}\left(\frac{T_s}{2A_{cor}}\right)^2 b_{cor}^2 \frac{s}{f_v A_v} = 0 \tag{9}$$

Further assuming that $B = \dfrac{f_{lb}A_{lb} + f_{lt}A_{lt} + f_{fl}A_{fl}}{b_{cor}}$, where f_{lb}, A_{lb} and f_{lt}, A_{lt} are the bottom and top longitudinal steel strength and area and f_{fl}, A_{fl} are the longitudinal FRP strip strength and area, the above-mentioned equilibrium equation is formed as:

$$\frac{\dfrac{T_s^2}{8A_{cor}^2 B}}{3A + \dfrac{s}{f_v A_v}} + \frac{\dfrac{V_s^2}{8h_0^2 B}}{3A} + \frac{\dfrac{T_s V_s}{4A_{cor}h_{cor}B}}{3A} = 1 \tag{10}$$

In consideration of $V_{u0}^2 = \dfrac{8h_0^2 B}{3A}$ without torsion but $T_{u0}^2 = \dfrac{8A_{cor}^2 B}{3A + \dfrac{s}{f_v A_v}}$ in pure torsion,

consequently, the correlative equilibrium equation of torque and shear at mode-2 type of failure (Krishna, 2003) can be derived as:

$$\frac{T_s^2}{T_{u0}^2} + \frac{V_s^2}{V_{u0}^2} + \frac{2T_s V_s}{T_{u0}V_{u0}\sqrt{\dfrac{4}{3} + \dfrac{f_{fs}A_{fs}s}{3f_v A_v s_f}}} = 1 \tag{11}$$

In solving the equations mentioned above, it is necessary to determine the effective strain of FRP sheet. The *fib* (*fib*, 2001)provisions on the shear strengthening of RC beams are built on the regression of experimental test results achieved by Triantafillou and Antonopoulos (Triantafillou and Antonopoulos, 2000). In the *fib* (*fib*, 2001)model, effective strain is governed by the FRP strengthening configuration, that is, effective strain is a function of the concrete compressive strength f_c' and the FRP axial rigidity ($E_f \rho_f$). For U-shaped CFRP jackets, the effective strain of the CFRP function is derived as follows:

$$\varepsilon_{fe} = 0.65\left(\frac{f_c'^{2/3}}{E_f \rho_f}\right)^{0.56} \times 10^{-3} \text{ For debonding} \tag{12a}$$

$$\varepsilon_{fe} = 0.17\left(\frac{f_c'^{2/3}}{E_f \rho_f}\right)^{0.30} \varepsilon_{fu} \text{ For fracture} \tag{12b}$$

where E_f is the modulus of elasticity of the CFRP in GPa, f_c' is the compressive strength of concrete in MPa, and ε_{fu} is the ultimate strain of the CFRP. With regard to

the U-shaped strips without longitudinal strips, debonding governed the failure, and the effective strain can use Eq. (12a). However, for U-shaped strips with longitudinal strips, Eq. (12b) can be utilized in the longitudinal CFRP strip.

4.4 Comparison with the Experimental Values

Because of very few experimental studies on reinforced concrete box beam strengthened by FRP subjected to torsion and shear, the values were obtained just from this paper and the literature (Li *et al*., 2005).The ultimate torque of the beams from the tests and calculation is showed in Figure 10. The horizontal ordinate and vertical ordinate stand for experimental and calculational values, respectively. The calculational result from this experiment reveals slightly more conservative than those from literature(Li *et al*., 2005), but the ultimate torques from the experimental results and the derived equations show a close agreement.Although combined action to obtain desirable results, a lot of experimental values should be gained to make the further verification.
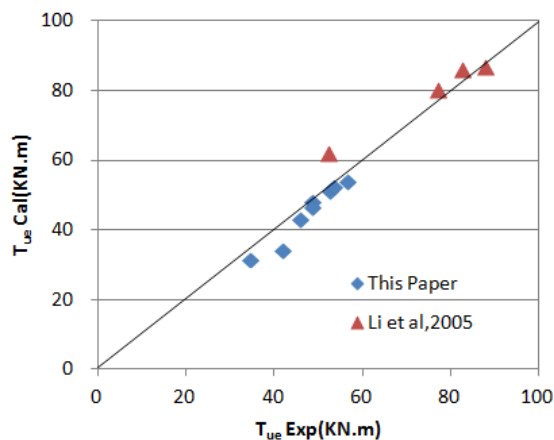

Figure 10: Calculation torque by derived equations compared with experimental values

5.0 Conclusions

Through investigating and analyzing the experimental results, the ultimate torque equations of RC box beam strengthened by CFRP under torsion and shear were derived. The conclusion can be achieved and listed as follows.

1. A reformed and innovated test setup with one hydraulic actuator providing different torque-to-shear ratios worked well in this study.
2. Based on the variable-angle truss model and mode-2 type of failure (Krishna, 2003) as well as shear flow, and equilibrium of forces and moment, the equations for calculating the ultimate torque of the box beams strengthened by CFRP were

derived. In addition, for U-shaped CFRP jackets, the effective strain of CFRP from the *fib* (*fib*, 2001) model was adopted under two main patterns of failure (debonding and fracture).

3. Existing experimental results were used in verifying the derived equations. The experimental and calculational values show a close agreement from Figure 10. The calculational result from this experiment, however, reveals slightly more conservative than those from literature(Li *et al*., 2005).

4. Desirable results can be gained from the derived equations calculating the ultimate torque of the strengthened beam under combined action, but more experimental studies should be conducted to make further verification.

5. From the experimental investigation, the cracking capacity of the box beams strengthened by CFRP was not improved noticeably, and the maximum increase was 4.1% for 2BBSL2 compared with the control beam. However, ultimate strength increased significantly, and the configuration of the U-jacket strips with longitudinal strips was more effective than that of the U-jacket without the longitudinal strips, which can change the failure mode from debonding to fracture. Therefore, good incremental percentages in ultimate torque of 51.8% for 2BBSL2 and 34.3% for 1BBSL2 were obtained. The ultimate torque of the beams strengthened by two layers of U-jacket strips with longitudinal strips was not proportional to that of the beams strengthened by one layer.

6. With the increase in torque-to-shear ratio, the effect of strengthening the box beams by CFRP decreased because U-jacket strips were less effective in torsional strengthening, but stirrups can play a more efficient role because the torsional behavior occupied more strength of the stirrup.

6.0   Acknowledgements

References

Attari, N., Amziane, S. & Chemrouk, M. (2012). *Flexural strengthening of concrete beams using CFRP, GFRP and hybrid FRP sheets*. Construction and Building Materials 37:746-757.

Al-Mahaidi, R., and A. K. Y. Hii. (2007).*Bond behaviour of CFRP reinforcement for torsional strengthening of solid and box-section RC beams*. Composites Part B: Engineering 38:720-731.

Ameli, M., and H. R. Ronagh. (2007).*Analytical method for evaluating ultimate torque of FRP strengthened reinforced concrete beams*. Journal of Composites for Construction 11:384-390.

Baggio, D., Soudki, K. & Noël, M. (2014). *Strengthening of shear critical RC beams with various FRP systems.* Construction and Building Materials 66:634-644.

Chalioris, C. (2007).*Behavioural model of FRP strengthened reinforced concrete beams under*

torsion. Asia-Pacific Conference on FRP in Structures ,Hongkong,China.111-116.

Chalioris,C.E. (2008).*Torsional strengthening of rectangular and flanged beams using carbon fibre-reinforced-polymers–Experimental study*. Construction and Building Materials 22:21-29.

Chen, G. M., J. F. Chen, and J. G. Teng. (2012).*On the finite element modelling of RC beams shear-strengthened with FRP*. Construction and Building Materials 32:13-26.

Deifalla, A., and A. Ghobarah. (2010).*Strengthening RC T-beams subjected to combined torsion and shear using FRP fabrics: Experimental study*. Journal of Composites for Construction 14:301-311.

Dong, J., Q. Wang, and Z. Guan. (2013).*Structural behaviour of RC beams with external flexural and flexural–shear strengthening by FRP sheets*. Composites Part B: Engineering 44:604-612.

fib, 2001, Externally bonded FRP reinforcement for RC structures: Lausanne, Switzerland,.

Ghobarah, A., M. Ghorbel, and S. Chidiac. (2002).*Upgrading torsional resistance of reinforced concrete beams using fiber-reinforced polymer*. Journal of composites for construction 6:257-263.

Hsu, T. T., and Y. Mo. (1985).*Softening of Concrete in Torsional Members-Theroy and Tests*. ACI Journal Proceedings 82.

Jing, M., and J. Grünberg. (2006).*Mechanical analysis of reinforced concrete box beam strengthened with carbon fiber sheets under combined actions*. Composite Structures 73:488-494.

Jing, M., W. Raongjant, and Z. Li. (2007).*Torsional strengthening of reinforced concrete box beams using carbon fiber reinforced polymer*. Composite Structures 78:264-270.

Krishna, R. N., 2003, Reinforced Concrete Design: Principles And Practice, New Age International.

Lampert, P., and Thurlimann, B. (1968).*Torsion Tests of Reinforced Concrete Beams*. Bericht No. 6506-2, Institute fur Baustatik, ETH, Zurich.

Li, Z., J. Meng, S. Biao, and W. Xiucun. (2005).*Model Experiments on Torsional Behavior of Carbon Fiber Sheet Strengthened RC Box Beams Subjected to Combined Action of Bending-Shear-Torsion*. China Civil Engineering Journal 12:38-44.

Panchacharam, S., and A. Belarbi. (2002).*Torsional behavior of reinforced concrete beams strengthened with FRP composites*. First FIB Congress, Osaka, Japan.1-11.

Shengqiang Ma, N. Muhamad Bunnori & Choong, K. K. (2015). *Experimental Study on Reinforced Concrete Box Beam Strengthened by CFRP under Combined Action*. Applied Mechanics and Materials 802: 184-189.

Triantafillou, T. C., and C. P. Antonopoulos. (2000).*Design of concrete flexural members strengthened in shear with FRP*. Journal of Composites for Construction 4:198-205.